STUDY ON VIBRATION ADSORPTION CHARACTERISTICS OF SMALL-PARTICLE-SIZE SEEDS BASED ON DEM
/
基于 DEM 的小粒径种子振动吸附特性研究

Wenxue DONG[1)], Na LI[1)], Fei LIU[*1)], Xuan ZHAO[1)], Lihe WANG[1)], Dezheng XUAN[1)], Wendong ZHONG[1)], Hengtong HU[1)], Xiang KONG[1)], Xinyu MENG[1)], Mingyi LI[1)], Zhijiang DUAN[1)]

[1)] College of Mechanical and Electrical Engineering, Inner Mongolia Agricultural University, Hohhot 010010, China;

Tel: 13238446338; E-mail: dong18403045597@163.com; afei2208@imau.edu.cn

DOI: https://doi.org/10.35633/inmateh-71-35

Keywords: *vibration; discrete element method; air-suction seed metering; seed-suctioning performance*

ABSTRACT

In order to explore the effect of vibration on the adsorption characteristics of small particle size seeds, based on the discrete element method, the changes in the variance of the average tangential force of seeds under different amplitudes were analyzed. The variance of the average tangential force of the seeds increases exponentially with the amplitude. It is inferred that the vibration will change the intensity of the population disturbance. This reduces the seed transient tangential force i.e. transient seed internal friction. To improve the adsorption characteristics of small-sized seeds, the adsorption characteristics at different amplitudes were verified with bench tests. Increasing the amplitude can improve the adsorption characteristics of small-sized seeds. To determine the optimal operating parameters, based on the Box–Behnken test principle, response surface tests were carried out using rotational speed, negative pressure, and amplitude as test factors and seed suction compliance and leakage rate as evaluation indexes. The optimum operating parameters were determined as: rotational speed of 12.05 r/min, negative pressure of 0.89 kPa, and amplitude of 5.75 mm. At this time, the seed suction pass rate was 95.1% and the leakage rate was 2.1%. which is in line with the standard requirements.

摘要

为探究振动对小粒径种子吸附特性的影响，基于离散元法，分析不同振幅下种子平均切向力方差的变化。种子平均切向力方差随振幅呈指数增加，据此推断振动会改变种群扰动强度，从而降低种子瞬态切向力即瞬时种子内摩擦力，以此提高种子吸附特性；通过台架试验验证不同振幅下的吸附特性，增大振幅可改善吸种特性。基于 Box-Behnken 试验原理，以转速、负压和振幅为试验因素，以吸种合格率和漏吸率为指标，进行响应面试验，确定最佳工作参数为：转速为 12.05 r/min，负压为 0.89 kPa，振幅为 5.75 mm，此时吸种合格率为 95.1%，漏吸率为 2.1%，符合标准要求。

INTRODUCTION

Air-suction seed-metering devices have high seeding precision and are widely used for crop seeding *(Zhang K. et al., 2017)*. A functioning seed dispenser causes vibrations that significantly affect the motion state of the seed population inside the seed chamber, while the motion state and degree of dispersion of the seed population directly affect the seed dispenser's seed-suctioning performance, which, in turn, affects the sowing accuracy *(Arzu Y. et al., 2014; Shi S. et al., 2015; Karayel D., 2022)*. Vibration during the sowing operation causes the seed population to have a certain speed, which leads to the phenomena of leakage and multiple sucking in the seed-sucking process and increases the variability of the seed sucking, affecting the seeding quality *(Yazgi A. et al., 2007; Ku s et al., 2021; Sakaguchi E. et al., 2001; Emrah Kus., 2021)*. When the vibration is larger, the seed population is more discrete, and the internal friction between seeds is smaller; however, due to the rapid movement of the population, the seeds are difficult to be adsorbed, resulting in a high leakage rate. Conversely, when the vibration is smaller, the seed population is less discrete, the internal friction between seeds is larger, the movement of the seed population is smaller, and the mobility of the seed population is poor, resulting in a high leakage rate. With an appropriate vibration, the seed population can reach the leakage rate of a relatively low state of "boiling" *(Liao Y.T. et al., 2022; Aliiev E. et al., 2019 ; Muhammad D. et al., 2021; Igor S. et al., 2021)*.

Vibration can cause the population to enter a "boiling" state due to the arrangement defects between the seeds in the population. The intensity of the vibration affects the "boiling" state of the seed population and, thus, the performance of seed adsorption. Medium-frequency vibration can make the seed population produce a "boiling" movement conducive to seed suctioning, wherein a low negative suction pressure can realize a high suction rate of qualified seeds *(Cujbescu D. et al., 2021; Zheng J. et al., 2023; Zhao X. et al., 2023; Wang B. et al., 2023)*.

One of the most common methods used to study the seeding process is DEM simulation analysis *(Lysych M.N. et al., 2021; Guzman L.J., 2020; Sharaby N.N. et al., 2020)*. *Chen et al. (2011)* further investigated the effects of different frequencies, amplitudes, and seed layer thicknesses on the spatial distribution of populations using EDEM software and determined the range of seed layer thicknesses favorable for the population's "boiling". *Hu et al. (2014)* analyzed the effects of vibration frequency and amplitude on the population movement pattern and seed supply performance based on the discrete element method, verifying them using high-speed photography technology and bench tests, and the simulation results coincided with the actual results. *Lu et al. (2016)* simulated and analyzed the homogenization process of a vibratory homogenizing device using the discrete element method and carried out experimental verification, and the verification results had a relatively small error with the simulation results, further confirming the discrete element method's high feasibility and accuracy.

Although the study determined the effect of vibration on the pneumatic seed discharger law, this law mainly applies to corn, rice, and other large-particle-size seeds. While quinoa and other small-particle-size (with an average diameter of less than 3 mm) pneumatic seed dischargers are the subjects of less relevant research. Quinoa is recognized as one of the world's most nutritious food crops with strong international market demand. Therefore, the effect of vibration on the stress and adsorption properties of small-particle-size populations should be studied using quinoa seeds as an example. In this paper, a quinoa seed contact model was developed based on the EDEM discrete element method. The force on quinoa seeds in the seed discharger under vibration was simulated and analyzed. The simulation results were verified using an indoor bench. In addition, a response surface test was designed using Design-Expert software. The optimal combination of working parameters was determined.

MATERIALS AND METHODS

Seed discharger structure and working principle

The seed discharger comprised a seed discharge shaft, air chamber, air chamber pressure plate, bushing, seed disk and shell, and other components, as shown in Figure 1. In this case, there were 18 clusters of suction holes distributed around the circumference of the seed disk, and each cluster contained four suction holes with a diameter of 0.8 mm for the adsorption of seeds. The seed tray was fixed to the seed discharge shaft and rotated in synchronization with the seed discharge shaft. The seed tray and the housing formed a seed chamber for storing the seeds.

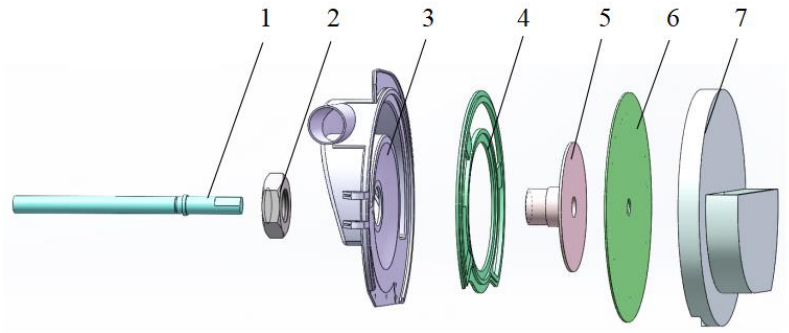

Fig. 1 - Structural diagram of air-suction seed metering

1. seed dispenser shaft; 2. fixing nut; 3. air chamber; 4. air chamber platen; 5. assortment tray; 6. assortment tray; 7. clamshell

The seed discharge device functions as follows: the seed discharge tray operates with the seed discharge axis under synchronous rotation. With the air chamber located outside the wind machine, when the vacuum in the air chamber reaches a certain negative pressure value, the seeds in the air chamber by the seed tray suction hole under the adsorption force overcome their own gravity and the friction between the seeds, and are ultimately adsorbed through the seed tray suction hole into the seed tray.

Due to the small size of the suction hole and the rotation of the seed tray, the suction hole can only carry out the stabilized adsorption of one seed, rather than using part of the suction hole as in the case of multiple suction. In a multi-suction situation, only one seed is stably adsorbed, and the adsorption force acting on the other seeds is less than their own gravity, which causes them to fall back into the seed chamber. Meanwhile, the adsorbed seed in the seed disk travels through the seed-carrying area to reach the seeding area, where the adsorption force disappears, and the seed falls into the ridge along the seed-guiding tube to complete the precise amount of seed discharge, as shown in Figure 2.

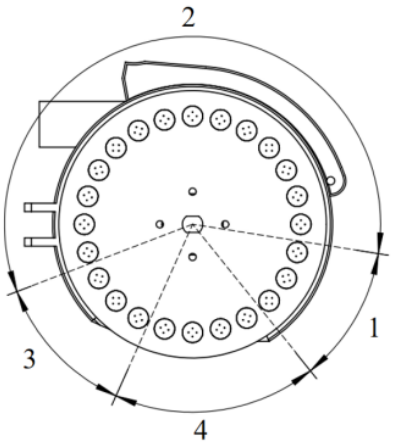

Fig. 2 - Working principle diagram of seed metering

1. seed dispersal area; 2. seed-holding area; 3. seed-dispensing area; 4. transition area.

Particle contact motion analysis

(1) Contact model

The discrete element method is used to simulate the collision process between particles, and these particles generate a contact force during the collision process. The contact force of soft-particle contact, an important contact model in the discrete element method, can be calculated according to the overlap between particles and the tangential relative displacement between particles, and the contact force between particles is closely related to internal friction. Therefore, this paper adopted the soft-particle contact model to simulate seed contact. Since there is no adhesion on the surfaces of quinoa seeds, the Hertz–Mindlin no-slip contact model was selected in this paper.

The damped motion of a spring oscillator was utilized to describe the contact process between the seeds, as shown in Figure 3, with the following equation of motion:

$$m\frac{d^2x}{dt^2} = -kx - \gamma\frac{dx}{dt} \quad (1)$$

where: x is the displacement from the equilibrium position, mm; m is the oscillator mass, g; k is the coefficient of spring elasticity; and γ is the spring damping factor.

In the normal direction, couplers are set to indicate seed contact without introducing any force, and sliders are set to achieve tangential sliding between seeds.

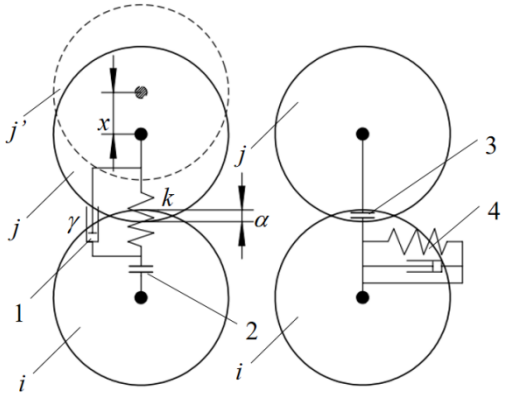

Fig. 3 - Soft-particle contact reduction model

1. shock absorbers; 2. coupler; 3. sliders; 4. spring; α is the normal overlap; γ is the spring damping factor; 2. k is the coefficient of spring elasticity; x is the displacement from the equilibrium position; and i and j are the seeds.

(2) **Contact force calculation** shows the force diagram of the seed contact process. In addition to its own gravity, a seed is also subjected to the normal and tangential forces generated by its contact with other seeds.

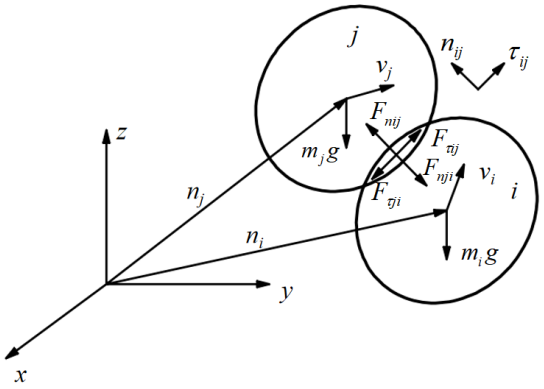

Fig. 4 - Seed contact process stress diagram

F_{nij} is the normal force on seed j; F_{nji} is the normal force on seed i; $F_{\tau ij}$ is the tangential force on seed j; $F_{\tau ji}$ is the tangential force on seed i; m_jg is the gravitational force on seed j; m_ig is the gravitational force on seed i; v_j is the velocity of seed j; v_i is the velocity of seed i; n_j is the center vector position of seed j; and n_i is the center vector position of seed i.

The normal force F_{nij} is the combined elastic and damping force acting on seed i by the spring and the normal damper. For three-dimensional spherical particles, according to the Hertz contact theory, F_{nij} is expressed as:

$$F_{nij} = (-k_n \alpha^{\frac{3}{2}} - \gamma_n v_{ij} \cdot n)n \tag{2}$$

where:

k_n is the normal elasticity coefficient; γ_n is the normal-phase damping factor; n is the unit vector from the sphere center of seed i to the sphere center of seed j; and v_{ij} is the velocity of seed i relative to seed j, m/s.

The tangential force is expressed as:

$$F_{\tau ij} = -k_\tau \delta - \gamma_\tau v_{\gamma\tau} \tag{3}$$

where:

K_τ is the tangential elasticity coefficient; δ is the tangential displacement of the point, m; γ_τ is the tangential damping coefficient; and $v_{\gamma\tau}$ is the contact slip speed, m/s.

When slip occurs on seed i, the following relationship exists:

$$\left|F_{\tau ij}\right| > \mu \left|F_{nij}\right| \tag{4}$$

At this point, the tangential force is:

$$\left|F_{\tau ij}\right| = -\mu \left|F_{nij}\right| n_\tau \tag{5}$$

where:

μ is the seed friction factor, and n_τ is the tangential unit vector.

Equation (5) is Cullen's friction law *(Li H.C. et al., 2011; Zhao Y.M. et al., 2006; Maroues F. et al., 2016)*, it can be seen from Eq.5 that the tangential force on the seed is the internal friction between the seeds. The tangential force on the seeds is the main factor that prevents the seeds from moving relative to each other or having a tendency to move relative to each other. Its magnitude is determined by the seed friction factor and normal force. The seed friction factor is a unique property. It remained essentially the same under the same test conditions. Therefore, in this paper, the internal friction between seeds is measured by the tangential force $F_{\tau ij}$.

Air-suction seed metering are subject to airflow disturbances during the seed filling process. A coupled gas-solid two-phase flow (DEM-CFD) simulation method is usually used for such systems where airflow and particles coexist. For CFD (fluid dynamics methods), vibration causes the airflow to change in size and direction. This change affects the simulation test results. And in the physics experiment, the vibrations did not change the size or direction of the airflow.

Shi et al. (2015) found that the airflow disturbance factors could be approximated as being at the same level at the time of the test by a one-factor comparison. Therefore, in this paper, the airflow disturbance factors are approximated to be controlled at the same level. In this way, the effect of perturbation intensity with different amplitudes on the adsorption characteristics of small-sized seeds was investigated.

Test materials and equipment

(1) Simulation modeling

The seed dispenser was modeled using SolidWorks software and imported into EDEM as shown in Figure 5.

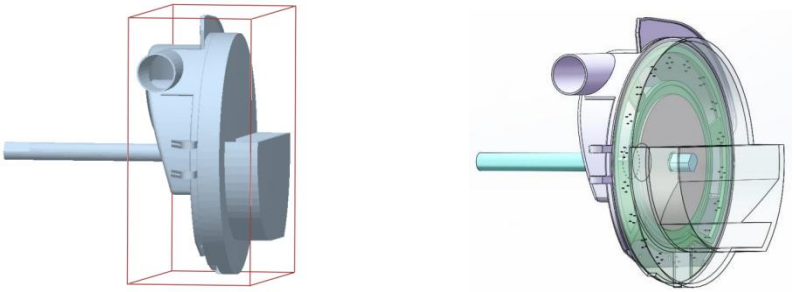

(a) SolidWorks model (b) EDEM model

Fig. 5 - Three-dimensional model of seed dispenser

In this paper, the seeds of Meng quinoa No. 1 were selected for the test, as shown in Figure 6(a). The simulation assumed that the external dimensions of the seeds were all the same due to the small size of the seeds and the low variability between the seeds. Firstly, the quinoa seeds were scanned and sampled with a Teng Yue intelligent industrial-grade 6.3 million-industrial-grating automatic 3D stereo scanner to obtain the quinoa seed model, as shown in Figure 6(b), which was imported into the EDEM simulation software to be filled to obtain the quinoa seed model close to the real quinoa seed model, as shown in Figure 6(c).

(a) Quinoa seed (b) Scanned model (c) Mesh fill model

Fig. 6 - Quinoa seed model

(2) Parameter setting

The parameters of the simulation were determined based on the results of previous work *(Wu Y.S. et al., 2017; Li D.P., 2020; Xu X.M. et al., 2019)*, as shown in Table 1. The Hertz-Mindlin contact model was chosen for the simulation. Simulate the Riley Time Ministerial Percentage setting of 20%. Mesh size was 2 mm. The simulation set the number of seeds at 20000 seeds. The total simulation time was 2 s, and the data were recorded every 0.01 s.

Table 1

Discrete element simulation parameters

Parameter	Numerical Value
Quinoa Poisson's ratio	0.25
PLA Poisson's ratio	0.36
Young's modulus of quinoa (MPa)	390.00
Young's modulus of PLA (MPa)	2350.00
Density of quinoa (g/cm^3)	0.87
Density of PLA (g/cm^3)	1.23
Quinoa–quinoa crash recovery factor	0.38
Quinoa–PLA crash recovery factor	0.50
Quinoa–quinoa static coefficient of friction	0.47
Quinoa–PLA static coefficient of friction	0.49
Quinoa–quinoa rolling coefficient of friction	0.12
Quinoa–PLA rolling coefficient of friction	0.11

To investigate the pattern of variation in the tangential forces on the seeds at different amplitudes, simulations were conducted with amplitude as the test factor and the vibration frequency of the seed discharger set at 10.7 Hz, the rotational speed of the seed discharger at 15 r/min, and the amplitude of the seed discharger at 0, 2, 4, 6, 8, and 10 mm *(Liu Y.Q., 2017)*.

Bench test conditions

The test seeds were selected from "Mengqua 1" grown in Ulanchab, Inner Mongolia, China. Vibration bench tests were carried out using the JPS-12 computer vision seed dispenser test rig manufactured by Harbin Bona Technology Co Ltd in China and the LKD-P absorbing electromagnetic shaker produced by Guangdong Lijia Industry Co, as shown in Figure 7.

Fig. 7 - Seeding performance test bench

1. vibrating stand; 2. seed dispenser stand; 3. air-aspirated quinoa seeder; 4. Electromagnetic shaker; 5. JPS-12 computer vision seed arranger test bed.

The bench test took the qualified rate of seed adsorption and the leakage rate as the evaluation index, 250 data were recorded continuously, and each group of tests was repeated three times to obtain the average value. As per the relevant standard, the quinoa precision hole sowed 3~5 seeds per hole. During sowing, it was assumed that all the seeds adsorbed by the suction pore clusters fell into the hole of the monopoly and that the seeds adsorbed by each suction pore cluster fell into the same hole. Each suction hole group was set up with 4 suction holes. When the number of seeds adsorbed by a suction hole group was less than 3, it was classified as leakage, and when each suction hole group stably adsorbed 3-5 seeds, it was classified as qualified adsorption. The leakage rate and qualified rate were calculated based on this standard.

$$M = \frac{n_1}{N} \times 100\% \tag{6}$$

$$Q = \frac{n_2}{N} \times 100\% \tag{7}$$

where:

M is the qualified rate, %; Q is the leakage rate, %; n_1 is the number of pore groups qualified for adsorption, pcs; n_2 is the number of suction hole clusters with leakage suction, pcs; and N is the total number of recorded suction pore clusters, pcs.

Bench test

A one-factor test was performed to verify the accuracy of the simulation results. The speed of the vibrating seed discharger seed disk was set as 15 r/min, the vibration frequency of seed discharger as 10.7 Hz, the negative pressure as 1 kPa, and the amplitude as 0, 2, 4, 6, 8, and 10 mm. To find the optimal combination of operating parameters, the designing of the experiments was carried out using Design-Expert software, and the factor coding is shown in Table 2.

Table 2

Discrete element simulation parameters

Level	Test Factors		
	Speed A (r/min)	Negative pressure B (kPa)	Amplitude C (mm)
1	10	0.8	4
0	12.5	1.0	6
-1	15	1.2	8

RESULTS

Simulation test results

(1) Population movement state analysis

The population movement state map is shown in Figure 8. Without vibration, the population was close to the wall inside the seed chamber, the internal friction between seeds was high, and the seed-suctioning performance was relatively poor. With vibration, the seed population began to show a throwing motion, and with the increase in amplitude, this throwing motion became gradually more obvious, and the seed population appeared to be in a "boiling" state. In this state, with the fluctuation in the normal force on the seeds and the change in the internal friction between the seeds, the seed-suctioning performance could be improved.

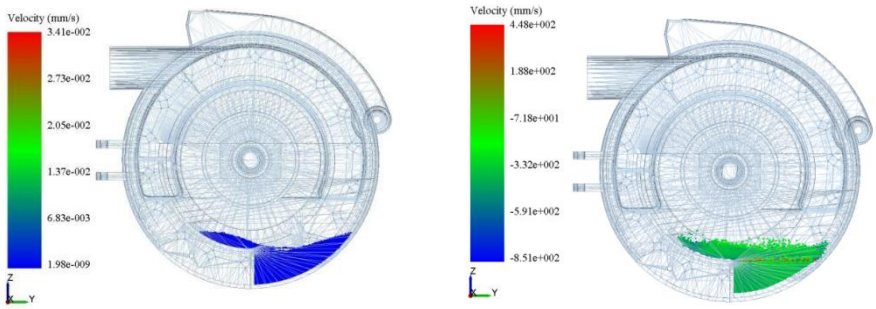

(a) Stationary stock (b) Population in boiling state

Fig. 8 - Population movement state map

(2) Normal force on seeds of different amplitudes

Using the EDEM software to output the total number of seeds, the total number of contacts, and the contact average normal force for each step, the average normal force f_{nt} applied to each seed at time t was:

$$f_{nt} = F_{nt} \frac{N_t}{N_{ct}} \tag{8}$$

where: F_{nt} is the average value of the contact normal force at time t, N; N_t is the total number of seeds at time t, grain; and N_{ct} is the total number of contacts at time t, grain.

Combine with equation (5) to calculate the average tangential force on the seed. The mean tangential force applied to the seeds at different amplitudes is shown in Figure 9. With vibration, the mean tangential force applied to the seeds appears to fluctuate irregularly, and the magnitude of the fluctuation increases with the increase in the amplitude.

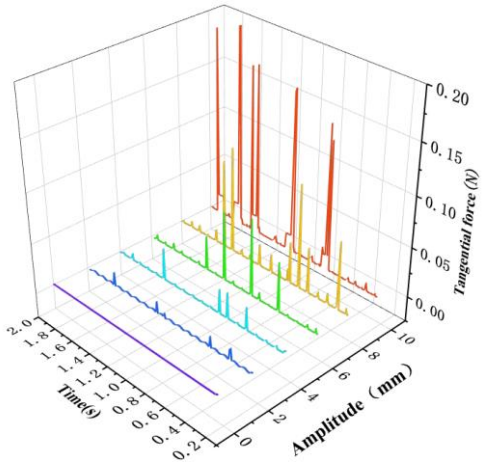

Fig. 9 - Average tangential force on seeds at different amplitudes

To quantitatively describe the fluctuation in the mean tangential force on the seeds, the variance formula is introduced with the following expression:

$$S^2 = \frac{1}{N_T} \sum (f_\pi - \frac{M_T}{N_T}) \tag{9}$$

$$M_T = \sum f_\pi \tag{10}$$

where:

S^2 is the variance; N_T is the total number of output data, N_T = 20000 grain; and M_T is the seed mean tangential force sum, N.

Figure 10 shows the pattern of the effect of amplitude on the seed tangential force. The seed mean tangential force variance increased exponentially with the amplitude, and when the variance was larger, the tangential force fluctuation was more discrete, and the fluctuation in the internal friction between seeds was larger, which improved the seed adsorption performance. The variance was highest when the amplitude was 10 mm, when the seeds were "boiling" violently in the seed chamber, which is unfavorable for seed adsorption. Therefore, an appropriate amplitude can change the internal friction between seeds, which, in turn, improves the seed-suctioning performance.

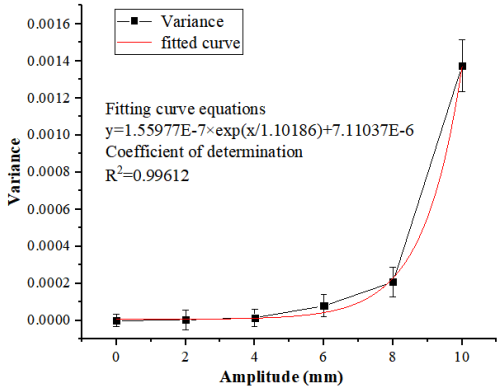

Fig. 10 - Effect of amplitude on variance in tangential force

Results and analysis of single factor test

The effect of amplitude variation on the seed adsorption performance is shown in Figure 11. As demonstrated in the figure, with the increase in the amplitude, the qualified rate of seed suctioning first shows a rising and then a falling trend. The leakage rate first shows a falling, then rising, falling, and, finally, sharply rising trend. Theoretically, the leakage rate at an amplitude of 4 mm should be less than at 6 mm. The phenomenon shown in Figure 11 may be due to variations in the number of seeds within the species chamber and experimental errors. When the amplitude was small, the effect of vibration on the population was small, and the internal friction between species was relatively large, which was not conducive to the population "boiling". With the increase in the amplitude, the effect of vibration on the population increased, and the friction between the species decreased, which was conducive to the population "boiling". As such, the leakage rate gradually decreased, thereby improving the seed-suctioning performance. However, the population "boiling" intensified with the further increase in the amplitude, so the seed speed at the suction hole was faster, and the original adsorption of seeds via the intense "boiling" of seed collisions fell, resulting in an increased leakage rate.

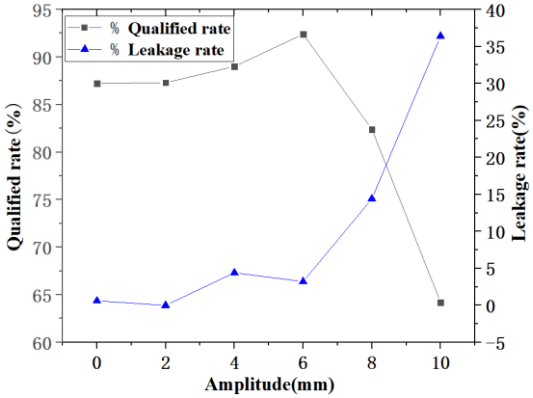

Fig. 11 - Seed adsorption performance curves at different amplitudes

Response surface test results and analysis

The experimental design was carried out using Design-Expert software, and the experimental protocol and results are shown in Table 3.

Table 3

Experimental design program and results

Test Number	Test Factors			Test Indicators	
	A	B	C	Qualified Rate Y_1 (%)	Leakage Rate Y_2 (%)
1	0	-1	1	84.7	12.6
2	1	1	0	85	12.4
3	0	0	0	93.4	2.2

Test Number	Test Factors			Test Indicators	
	A	B	C	Qualified Rate Y_1 (%)	Leakage Rate Y_2 (%)
4	-1	0	-1	86.3	3.6
5	0	1	-1	86.1	5.2
6	1	-1	0	88.6	4.1
7	-1	-1	0	90.5	6.2
8	1	0	1	81.9	15.3
9	-1	1	0	91.2	3.1
10	1	0	-1	81.1	8.1
11	0	1	1	83.6	12.7
12	-1	0	1	81.2	13.4
13	0	-1	-1	90.3	3.2
14	0	0	0	95.1	2.4
15	0	0	0	94.6	3.6

The regression analysis of the test results by Design-Expert software is shown in Table 4.

Table 4

Analysis of variance table of test results

Source of Variance	Qualified Rate Y_1 (%)					
	Sum of Squares	Freedom	Mean Square	F-Value	P-Value	Significance
Model	327.53	9	36.39	41.31	0.0004	**
A	19.85	1	19.85	22.53	0.0051	**
B	8.41	1	8.41	9.54	0.0272	*
C	19.22	1	19.22	21.82	0.0055	**
AB	4.62	1	4.62	5.25	0.0706	
AC	8.70	1	8.70	9.88	0.0256	*
BC	2.40	1	2.40	2.73	0.1596	
A_2	82.00	1	82.00	93.07	0.0002	**
B_2	4.99	1	4.99	5.66	0.0632	
C_2	200.15	1	200.15	227.18	＜0.0001	**
Residuals	4.41	5	0.88			
Fail to fit	4.15	3	1.38	10.63	0.0872	
Error	0.26	2	0.13			
Total	331.94	14				
Source of Variance	**Leakage Rate Y_2 (%)**					
	Sum of Squares	Freedom	Mean Square	F-Value	P-Value	Significance
Model	310.26	9	34.47	70.96	＜0.0001	**
A	23.12	1	23.12	47.59	0.0010	**
B	6.66	1	6.66	13.71	0.0140	*
C	143.65	1	143.65	295.68	＜0.0001	**
AB	32.49	1	32.49	66.87	0.0004	**
AC	1.69	1	1.69	3.48	0.1212	
BC	0.90	1	0.90	1.86	0.2311	
A_2	26.83	1	26.83	55.23	0.0007	**
B_2	3.85	1	3.85	7.92	0.0374	*
C_2	80.55	1	80.55	168.81	＜0.0001	**
Residuals	2.43	5	0.49			
Fail to fit	1.28	3	0.43	0.75	0.6164	
Error	1.15	2	0.57			
Total	321.69	14				

e, 0.05 < P < 0.1; ** indicates highly significant, P < 0.01.

As demonstrated in the variance results, the rotational speed and amplitude of the two indicators were highly significant, the negative pressure had a significant effect on the leakage suction rate, some of the factors had a two-by-two interaction, the regression model fit of the two evaluation indicators was highly significant, and the misfit term P was > 0.05, which indicates that there were no other factors affecting the evaluation indicators. The regression model after removing insignificant factors was:

$$Y_1 = 92.64 + 1.92A + 2.39C + 1.48AC - 5.75A^2 - 5.01C^2 \quad (11)$$

$$Y_2 = 5.68 - 3.83A - 0.73B - 5.88C + 2.58AB + 5.39A^2 + 0.77B^2 + 3.71C^2 \quad (12)$$

Using the regression coefficient test, it was concluded that the factors affecting the pass rate were amplitude, rotational speed, and negative pressure in order of predominance, and the factors affecting the leakage suction rate were amplitude, rotational speed, and negative pressure in order of predominance.

Based on the regression equation, a surface plot of the effects of factors with significant two-by-two interactions on the evaluation indicators was drawn. As shown in Figure 12, the qualified seed suction rate was higher when the rotational speed was 11.9-12.3 r/min, the negative pressure was 0.89-0.94 kPa, and the amplitude was 5.7-6.1 mm. As shown in Figure 12, with the increasing rotational speed, the qualified seed suction rate first rose and then decreased. When the rotational speed is low, the seed travels via the suction hole through the suction zone for a longer time, and there is a hole in the case of multiple suctioning. While the rotational speed is high, the seed via the suction hole travels through the west central zone for a shorter time, and part of the seed is not adsorbed via the suction holes into the suction zone, resulting in a high suction leakage rate. With the increase in negative pressure, the qualified rate first rose slowly after a slow decline because the negative pressure range selected for the test was favorable for seed suctioning, so the negative pressure on the qualified seed suction rate was small. However, the leakage rate significantly impacted the suction rate, whereby the negative pressure was small when the leakage rate was high, and the negative pressure was large when the leakage rate was lower, and the suctioning hole phenomenon increased. With the increase in amplitude, the qualified seed suction rate first rose and then fell. An appropriate amplitude can change the amount of internal friction between seeds, which, in turn, improves the seed-suctioning performance.

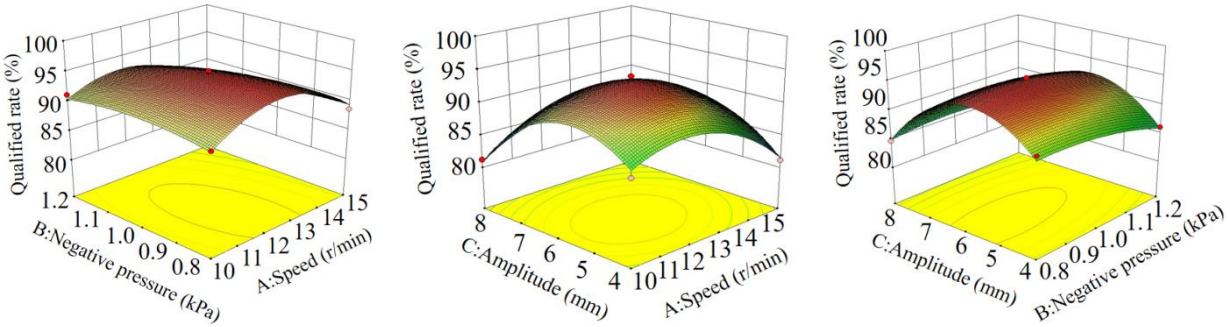

Fig. 12 - Effect of interaction on qualified rate

To obtain the best working parameters, a multi-objective optimization analysis was carried out using the Design-Expert software with a larger qualified rate and a smaller leakage suction rate as the objective function and the following objective function and constraints:

$$\begin{cases} \max Y_1(A,B,C) \\ \min Y_2(A,B,C) \\ \text{s.t.} \begin{cases} 10 \text{ r/min} \le A \le 15 \text{ r/min} \\ 0.8 \text{ kPa} \le B \le 1.2 \text{ kPa} \\ 4 \text{ mm} \le C \le 8 \text{ mm} \end{cases} \end{cases} \quad (13)$$

The optimal working parameters were calculated as follows: when the rotational speed of the seed discharger was 12.05 r/min, the negative pressure was 0.89 kPa, the amplitude was 5.75 mm, the qualified seed suction rate was 95.1%, and the leakage rate was 2.1%.

DISCUSSION

EDEM simulation was used to analyze the effect of vibration on the tangential force exerted on the seeds in the seed discharger. *Shi et al. (2015)* found that the airflow disturbance factors could be approximated as being at the same level at the time of the test by a one-factor comparison. It shows that the effect of airflow on the simulation results is acceptable.

In this study, the effect of airflow on seed tangential force was ignored during numerical simulation tests. The simulation results show that the average normal force on the seeds was stable and constant without vibration, resulting in relatively large inter-seed friction. As vibration causes seeds to produce a throwing motion, during the throwing process, the normal force between the seeds decreases and thereby reduces the internal friction between the seeds, which is favorable for seed suctioning. When the throwing process is over, the seeds in the bottom layer of the seed chamber collide with the seed chamber, and the seeds in other seed layers collide with each other, and the normal force increases instantly, i.e., the raised point of the curve in Fig. 10. The duration of this state is very short so it does not significantly affect the suctioning performance. When the vibration is too large, the seed throwing movement is intense, and the seeds pass through the suction hole at a faster speed, which is not conducive to seed suctioning. This agrees with the findings of *Lai et al. (2016)*.

The effects of different amplitudes on the seed adsorption performance are as follows: when the amplitude is small, the vibration of the population is small, and there is relatively high friction between the seeds, which is not conducive to the population "boiling". When the amplitude is large, the population "boiling" intensifies so the seed speed at the suction hole increases, and the original adsorption of the seeds via the intense "boiling" seed collision falls, resulting in an increased leakage rate. An appropriate amount of vibration can effectively reduce the internal friction between seeds and thus improve the qualified suction rate and reduce the leakage rate. If the vibration can be effectively reduced, it can be used to reduce the leakage rate. This is consistent with the findings of *Liao et al. (2022)*.

The results of the bench test show that the seed discharger worked with an amplitude within the range of 5.7-6.1 mm, and the seed suction pass rate was high, which is consistent with the results of the study by *Zhang et al. (2016).* Therefore, it is recommended that vibration be utilized to improve the seed-suctioning performance of small-particle-size air-aspirated seed dischargers.

CONCLUSIONS

In this study, the population movement was simulated using EDEM software, and the results were analyzed using the seed mean normal force variance as an indicator. It was concluded that proper vibration can reduce the internal friction between seeds and thus improve the seed-suctioning performance.

Taking the qualified seed suction rate and the leakage rate as indicators, a one-factor test was conducted on the amplitude, and the results obtained were consistent with those of the simulation analysis, which verified the correctness of the constructed contact model and the feasibility of using the discrete element method to simulate population movement.

A response surface test was used to analyze the rotational speed, negative pressure, and vibration, as well as some of the factors' two-by-two interactions with the indicators, to determine the optimal combination of operating parameters, detailed as follows: a rotational speed of 12.05 r/min, negative pressure of 0.89 kPa, amplitude of 5.75 mm, of the qualified seed suction rate of 95.1%, and suction leakage rate of 2.1%.

In subsequent studies, vibration can be used to improve seed-suctioning performance by adding excitation or damping devices, damping when the operating amplitude is large, and adding excitation when the operating amplitude is small. According to the optimal seed adsorption performance with the population movement and the size of the seed normal force, seed-stirring devices suitable for quinoa and other small-sized seeds can be designed so that the populations favor seed adsorption in a "boiling" state to improve the seed adsorption performance.

ACKNOWLEDGEMENT

This work was supported by the National Natural Science Foundation of China (32060418).

REFERENCES

[1] Aliiev, E., Gavrilchenko, A., Tesliuk, H. et al. (2019). Improvement of the sunflower seed separation process efficiency on the vibrating surface. *APTEFF*. 2019, 50, 1-352. DOI: https://doi.org/10.2298/APT1950012A.

[2] Arzu, Y., Adnan D. (2014). Measurement of seed spacing uniformity performance of a precision metering unit as function of the number of holes on vacuum plate. *Measurement*. 56, 128-135. DOI:10.1016/J.MEASUREMENT.2014.06.026.

[3] Chen, J., Zhou, H., Zhao, Z. et al. (2011). Analysis of Rice Seeds Motion on Vibrating Plate Using EDEM. *Transactions of the Chinese Society of Agricultural Machinery*. 42, 79-83+100.

[4] Cujbescu, D., Găgeanu, I., Persu, C. et al. (2021). Simulation of Sowing Precision in Laboratory Conditions. *Appl. Sci.* 11, 6264. https://doi.org/10.3390/app11146264.
[5] Emrah, K. (2021). Field-scale evaluation of parameters affecting planter vibration in single seed planting. *Measurement*. 184,109959. DOI:10.1016/J.MEASUREMENT.2021.109959.
[6] Guzman, L.J., Chen, Y., Landry, H. (2020). Discrete element modeling of seed metering as affected by roller speed and damping coefficient. *Transactions of the ASABE*. 63(1):189-198.
[7] Hu, J.P. Guo, K. Zhou, C.J. et al. (2014). Simulation and Experiment of Supplying Seeds in Box of Magnetic Precision Cylinder-seeder. *Transactions of the Chinese Society of Agricultural Machinery*. 45, 61-65.
[8] Ibrahim, E.J., Elfadil, A.D., Abdallah, A.D. (2022). Laboratory and Field Investigation Comparison for Seed Distribution Accuracy of a Multi-Rows Pneumatic Plate Metering Device. *Asian Journal of Agriculture and Food Sciences*. Volume 10-Issue 2. DOI:10.24203/ajafs.v10i2.6942.
[9] Igor, S., Elchyn, A., Gintas, V. et al. (2021). Modeling Separation Process for Sunflower Seed Mixture on Vibro-Pneumatic Separators. *Mechanika*. Volume, 27(4):311-320.
[10] Karayel, D., Güngör, O., Šarauskis E. (2022). Estimation of Optimum Vacuum Pressure of Air-Suction Seed-Metering Device of Precision Seeders Using Artificial Neural Network Models. *Agronomy* 12,1600. https://doi.org/10.3390/agronomy12071600.
[11] Ku, S.E. (2021). Field-scale evaluation of parameters affecting planter vibration in single seed planting. *Measurement*. 184,109959. DOI:10.1016/J.MEASUREMENT.2021.109959.
[12] Li, D.P. (2020). Discrete element analysis and performance test of pneumatic precision metering device for quinoa. *Inner Mongolia Agricultural University*.
[13] Lu, F.Y., Ma X., Qi L. et al. (2016). Parameter optimization and experiment of vibration seed-uniforming device for hybrid rice based on discrete element method. *Transactions of the Chinese Society of Agricultural Engineering*. 32,17-25. Doi:10.11975/j.issn.1002-6819.2016.10.003.
[14] Li, H.C., Li Y.M., Tang, Z. et al. (2011). Numerical simulation and analysis of vibration screening based on EDEM. *Journal of Agricultural Engineering*. 27, 117-121. Doi:10.3969/j.issn.1002-6819.2011.05.019.
[15] Liao, Y.T., Qi, T.X., Liao, Q.X. et al. (2022). Vibration characteristics of pneumatic combined precision rapeseed seeder and its effect on seeding performance. *Journal of Jilin University (Engineering Edition)*. 52, 1184-1196. Doi:10.13229/j. cnki. jdxbgxb20210001.
[16] Liu, Y.Q. (2017). Study on vibration characteristics of air suction no-tillage planter and its effect on seed metering performance. *Inner Mongolia Agricultural University*.
[17] Lysych, M.N., Chernyshev, V.V., Nagaytsev, V.M. (2021). Design and simulation of seed metering device for aerosowing of forest pelleted seeds. *Journal of Physics: Conference Series*. 2032,012062. DOI:10.1088/1742-6596/2032/1/012062
[18] Maroues, F., Flores, P., Claro, J. et al. (2016). A survey and comparison of several friction force models for dynamic analysis of multibody mechanical systems. *Nonlinear Dynamics*. 86, 1407. Doi:10.1007/S11071-016-2999-3.
[19] Muhammad, D., Rozzaq H.A., Makbul H. (2021). Multiobjective Optimization of Vibro-Pneumatic Separator Using Full Factorial Design. *Advances in Biological Sciences Research*. 19, 380-386. Doi:10.2991/absr.k.220305.059.
[20] Sakaguchi, E., Suzuki, M., Favier, J. F. et al. (2001). Numerical simulation of the shaking separation of paddy and brown rice using the discrete element method[J]. *Postharvest Technology*, 79(3): 307-315. DOI:10.1006/JAER.2001.0706.
[21] Sharaby, N. N., Doroshenko, A.A., Butovchenko, A. V. (2020). Simulation of Sesame Seeds Outflow in Oscillating Seed Metering Device Using DEM. *Inzhenerernyye tekh- nologii i sistemy = Engineering Technologies and Systems*. 30(2):219-231. DOI: https://doi.org/10.15507/2658-4123.030.202002.219-231.
[22] Shi, S., Zhang, D.X., Yang, L. et al. (2015). Simulation and verification of seed-filling performance of pneumatic-combined holes maize precision seed-metering device based on EDEM. *Transactions of the Chinese Society of Agricultural Engineering*. 31, 62-69. Doi: 10.3969/j.issn.1002-6819.2015.03.009.
[23] Wang, B., Liao, Q., Wang, L. et al. (2023). Design and Test of Air-Assisted Seed-Guiding Device of Precision Hill-Seeding Centralized Seed-Metering Device for Sesame. *Agriculture.* 13, 393. https://doi.org/10.3390/agriculture13020393.

[24] Wu, Y.S., Guo, Z.B., Du, W.L. et al. (2017). Study of the Material Properties on the Quinoa Threshed Mixture. *Journal of Agricultural Mechanization Research*. 39, 184-189. Doi:10.13427/j.cnki.njyi.2017.09.036.

[25] Xu, X.M., Li, F.X., Li, Y.X. et al. (2019). Design and Experiment of Quantitative Variable Pitch Screw. *Transactions of the Chinese Society of Agricultural Machinery*. 50, 89-97. Doi:10.6041/j.issn.1000-1298.2019.12.010.

[26] Yazgi, A., Degirmencioglu, A. (2007). Optimisation of the seed spacing uniformity performance of a vacuum-type precision seeder using response surface methodology. *Biosyst*. Eng. 97, 347–356. DOI:10.1016/J.BIOSYSTEMSENG.2007.03.013.

[27] Zheng, J., Liao, Y.T., Qi, T.X. et al. (2023). Effect of vibration on performance of pneumatic rapeseed precision metering device. *Journal of Huazhong Agricultural University*. 42, 233-242. DOI : 10.13300/j.cnki.hnlkxb.2023.02.029.

[28] Zhang K.; Yi S.J. (2017). Simulation and experimental optimization of seed filling performance of air-absorbing drum type corn seed discharger. *Transactions of the Chinese Society of Agricultural Machinery*. 48, 78-86. Doi: 10.6041/j.issn.1000-1298.2017.07.010 .

[29] Zhang, T., Liu, F., Zhao, M.Q. et al. (2016). Movement law of maize population in seed room of seed metering device based on discrete element method. *Transactions of the Chinese Society of Agricultural Engineering*. 32, 27-35. Doi:10.11975/j.issn.1002-6819.2016.22.004.

[30] Zhao, X., Zhang, T., Liu, F. et al. (2023). Sunflower Seed Suction Stability Regulation and Seeding Performance Experiments. *Agronomy.* 13, 54. https://doi.org/10.3390/agronomy13010054.

[31] Zhao, Y.M., Zhang, S.G., Jiao, H.G. et al. (2006). Simulation of discrete element of particles motion on vibration plane. *Journal of China University of Mining and Technology*. 586-590.